

# Ocean color variability in the Southern Atlantic and Southeastern Pacific

Natalia M. Rudorff<sup>\*a</sup>, Robert J. Frouin<sup>b</sup>, Milton Kampel<sup>a</sup>

<sup>a</sup>Divisão de Sensoriamento Remoto, Instituto Nacional de Pesquisas Espaciais,  
São José dos Campos, SP, Brazil,

<sup>b</sup>Scripps Institution of Oceanography, University of California San Diego, La Jolla, CA, USA

## ABSTRACT

The chlorophyll-*a* concentration (Chl<sub>a</sub>) of surface waters is commonly retrieved from space using an empirical polynomial function of the maximum band ratio (MBR), i.e., the maximum ratio of remote sensing reflectance in selected spectral bands in the visible. Recent studies have revealed significant deviations in the relation between MBR and Chl<sub>a</sub> across the oceans. The present work aims at accessing the main sources of MBR variability across the Southern Atlantic and South-east Pacific, using *in situ* data. The data was collected at 19 bio-optical CTD stations and 40 flow-through stations during a cruise onboard the R/V Melville, from South Africa to Chile (February-March, 2011). The MBR was derived from modeled remote sensing reflectance using absorption and backscattering measurements. The second order MBR variations (MBR\*) were obtained after subtraction of a global polynomial fit for Cl<sub>h</sub>a and Chl<sub>a</sub> biases. Multivariate analyses were used to explain the variations with bio-optical properties and phytoplankton pigments. Chl<sub>a</sub> overestimations were associated to high specific phytoplankton absorption (0.73), specific particle backscattering coefficient (0.42) and colored dissolved and particle organic matter (CDM) absorption normalized by non-water absorption (0.38), and vice-versa. The overestimations occurred at stations with dominance of small picoplankton, high concentration of bacteria, and high CDM, while underestimations were in microplankton dominated waters and low CDM. The results reveal important relations of the MBR\* with the specific coefficient and associated phytoplankton community structure.

**Keywords:** Maximum Band Ratio algorithm, chlorophyll\_*a* concentration, bio-optical variability, Southern Atlantic and South-east Pacific.

## 1. INTRODUCTION

The chlorophyll-*a* concentration (Chl<sub>a</sub>) of surface waters can be retrieved from space using an empirical polynomial function of the maximum band ratio (MBR), i.e., the maximum ratio of remote sensing reflectance in selected spectral bands in the visible, namely the OC4 model<sup>1</sup>. This empirical fit is adjusted with a global *in situ* data set of coincident measurements of remote sensing reflectance ( $R_{rs}$ ) and Chl<sub>a</sub>. The empirical fit has shown a good accuracy for Case 1 waters<sup>1</sup> where the biogenic components co-vary with the phytoplankton assemblage. The global data set is constantly updated with new *in situ* surveys, nevertheless there are still large unsampled areas across the oceans, which may compromise the retrieval in these areas and interpretations of the ocean colour variability<sup>3</sup>.

Through the polynomial function, the first order variation of the MBR is linked to the bulk phytoplankton biomass, indexed by the Chl<sub>a</sub>, and co-varying biogenic material. The deviations of the MBR vs. Chl<sub>a</sub> in respect to the global fit, are due partly to uncertainties regarding both measurements, and partly to second order variations of the bio-optical properties of the living and non-living assemblage of particles and dissolved substances<sup>4,5,6</sup>. For example, the different phytoplankton community structure, in terms of size, accessory pigment composition, intracellular pigment concentration, cell wall composition and shape, as well as, the bulk particle size distribution (PSD) (including detritus,

\*nmr@dsr.inpe.br; Tel: +55 (12)3208-6498; Fax: +55 (12)3208-6488

Remote Sensing of the Marine Environment II, edited by Robert J. Frouin,  
Naoto Ebuchi, Delu Pan, Toshiro Saino, Proc. of SPIE Vol. 8525, 85250N  
© 2012 SPIE · CCC code: 0277-786/12/\$18 · doi: 10.1117/12.981776

Proc. of SPIE Vol. 8525 85250N-1

hydrosols, minerals, bacteria and virus) and the coloured dissolved organic matter (CDOM) concentration. All of these constituents will determine the bulk optical properties of a specific sampling site, and any variation from the mean relation that links each of these with the Chla and MBR will result in a second order variation. Recent studies have shown that three specific optical properties may potentially cause significant deviations in the MBR model: e.g. the particle backscattering coefficient and phytoplankton absorption coefficient normalized by Chla, ( $b_{bp}^*$  and  $a_{phy}^*$ , respectively) and dissolved plus detritus coloured organic matter absorption ( $a_{cdm}$ ) normalized by the non-water absorption ( $a_{nw}$ ) ( $a_{cdm}^*$ )<sup>3,6</sup>. The first two are related to the efficiency of a particle to backscatter and absorb, respectively, in relation to each milligram of Chla, given in units of  $m^{-2}.mgChla^{-1}$  (cross section). The  $b_{bp}^*$  will essentially depend on the size, shape, concentration and refractive index of the particles, both living and non-living. High  $b_{bp}^*$  are usually associated to small spherical particles with low index of refraction<sup>7</sup>. The  $a_{phy}^*$  is a property that varies essentially with the phytoplankton cells and will depend primarily on how much each chlorophyll molecule is exposed to light or affected by shading effects due to chloroplasts organization and intracellular pigment concentration<sup>8</sup>. The higher the exposure, the higher absorbing capacity of each chlorophyll  $a$  and higher  $a_{phy}^*$ . In natural environments this variability also referred as “packaging effect” is generally associated to the size structure of the phytoplankton community<sup>8</sup>. Small picoplankton cells usually have low intracellular pigment concentration and high  $a_{phy}^*$ , while large microplankton have higher pigment concentration and lower  $a_{phy}^*$ . Other factors that may have minor but also significant effects on  $a_{phy}^*$  are the accessory pigments in relation to Chla and cell physiological state. The  $a_{cdm}^*$  is related to the variation of the CDOM and detritus concentration in respect to the phytoplankton community. The mean relation between CDOM and Chla in Case 1 waters and the deviations from this relation has recently received more attention for ocean colour studies, especially after the proposed CDOM index of Morel and Gentili<sup>5</sup>. It was thought that CDOM was supposed to present a relatively stable co-variation with Chla in Case 1 waters, however these studies have shown that there are significant deviations from the global mean relation, which are still not clearly understood. CDOM has two main origins: marine and continental and is a product of physical-chemical and biological degradation of detritus. The detritus is added to the CDOM term in ocean colour studies because they have a very similar spectral behavior which makes difficult the separation of each with radiometric measurements. The detritus is composed by non-living organic particles, mostly of degradation products. In coastal water there may also be a mineral fraction associated with the detritus from bottom re-suspension and river outflow. The different processes involved in the CDOM and detritus composition, i.e., zooplankton grazing, bacterial decomposition, photodegradation, fragmentation, and transport by currents and waves and upwelling cells will all affect the  $a_{cdm}^*$  of both oceanic and coastal waters. Thus, its variation is much more complex.

The identification of the second order variations of the MBR vs. Chla relation due to these specific bio-optical properties should help to improve the Chla OC4 retrieval, such as proposed by Morel and Gentili<sup>5</sup> for the CDOM deviation. The bio-optical variability is also a mean to study bio-optical provinces, relating the specific inherent optical properties (IOP) with the biogeochemical processes and phytoplankton community structure. The present work aims at contributing to such studies by analyzing the bio-optical variability across a region that has very few sampled points in the global ocean colour data sets: the Southern Atlantic and South-east Pacific. The data set consists of *in situ* radiometric and bio-optical measurements collected in the MV1102 cruise during the end of the austral summer of 2011. We investigate the possible sources of the second order variability on the MBR, in respect to bio-optical specific properties and their relation with indexes of the bacterial and phytoplankton community structure. In the end we present a synthesis of the bio-optical variability across the study region, linked to the distribution of indexes of the phytoplankton community.

## 2. MATERIAL AND METHODS

### 2.1 The MV1102 cruise and study area

Bio-optical and radiometric *in situ* data were obtained during a campaign onboard the R/V Melville (Scripps Institution of Oceanography, SIO) across the Southern Atlantic and Southeastern Pacific. The MV1102 departed from Cape Town, South Africa (34°S, 18°E) on February 19th, 2011, and arrived at Valparaiso, Chile (36°S, 76°W) on March 13th, 2011 (Figure 1). The cruise passed through important biogeochemical systems with a considerably high range of Chla from 0.07  $mg.m^{-3}$  to 5.0  $mg.m^{-3}$ . The first stations were collected in meso-eutrophic waters of the Benguella Upwelling Ecosystem (BEN) off the South African Coast. The vessel followed westward through low Chla waters of the South Atlantic Subtropical Gyre (SAG) and crossed mesotrophic waters of the South Atlantic Subtropical Convergence Zone (SACZ). The SACZ is characterized by sharp temperature-salinity and Chla gradients due to the penetration of high

nutrient low chlorophylla (HNLC) and cold-low salinity waters of the Southern Ocean, under warmer-higher salinity waters of the SAG. After 55°W, the MV1102 crossed meso-eutrophic waters of Patagonian Shelf Ecosystem (PSE), where HNLC waters of the Southern Ocean carried by the Malvinas Current meet iron enriched coastal waters, promoting high phytoplankton biomass growth<sup>9</sup>. The last sector sampled by the MV1102 was in the Pacific Southeast waters off the south Chilean coast (CC) up to 35°S. This sector is the most productive of the Chilean coast with meso-eutrophic waters, with evidences of intrusions of HNLC waters of the Southern Ocean that meet iron enriched coastal waters on the upper layer of the continental shelf<sup>10</sup>.

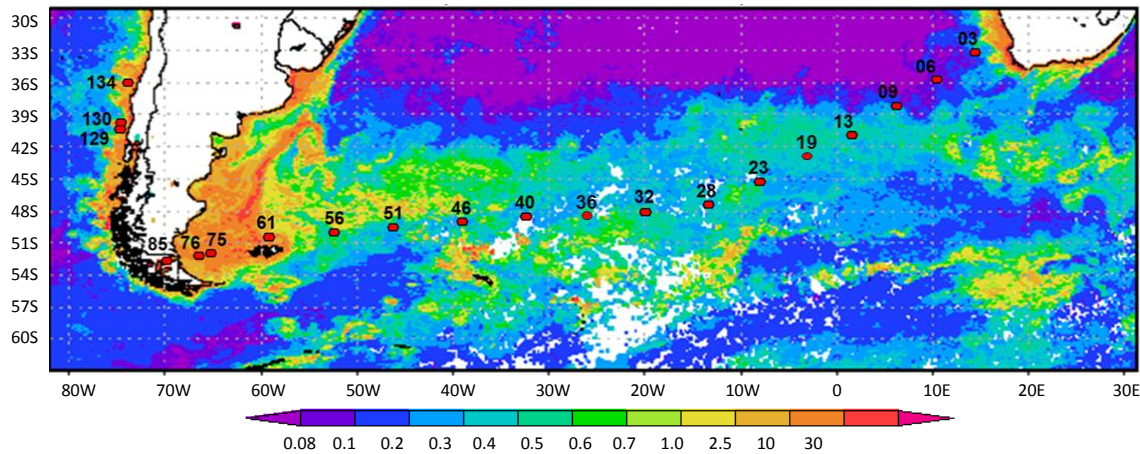


Figure 1: CTD stations shown in a MODIS (Moderate Resolution Spectroradiometer) 8 day composite (4 km) Chla map (log scaled in mg·m<sup>-3</sup>) during the MV1102 (02/18/11-03/06/11).

## 2.2 Data Collection and Processing

A total of 19 CTD stations were undertaken with radiometric and bio-optical measurements of the surface and vertical profile of the ocean upper layer, with collections around noon local time (11-13:00). Radiometric measurements were collected with the above and in-water radiometers: ASD Fieldspec Hand-Held (ASD Inc.) and HyperOCR II (Satlantic). The backscattering coefficient ( $b_b$ ) was determined with a Hydrosat-6S (HOBI labs Inc.) (H6S) deployed in a winched profiling system. Biogenic absorption, Chla, phytoplankton pigment composition, and picoplankton cell concentration were determined in water samples collected with a rosette bottle system, coupled with a CTD (Conductivity Temperature Depth), at 4 depths distributed in the sub-surface, chlorophyll maximum, and up to  $\approx 100$  m deep. Along the cruise track samples were also collected with the ship flow-through system (4 m deep) (referred as F1 stations), totalizing 40 sub-surface stations with a complete set of measurements of IOP (absorption and backscattering) and water constituents. For these stations the  $b_b$  was measured with the H6S in the water collected in a black bucket (60x40 cm). The CDOM absorption ( $a_s$ ) was measured onboard with a Cary 60 spectrometer. All other measurements were made after the cruise in separate laboratories, with adequate preservation of filtered samples in liquid nitrogen.

For the radiometric measurements the sampling and data processing schemes followed Mueller et al.<sup>11</sup>. The backscattering coefficient ( $b_b$ ) was processed using Hydrosot 2.9 following Dana and Maffione<sup>12</sup>. The ocean colour bands (443, 490, 510 and 555 nm) were determined using a power law fit (minimum square) to interpolate (and extrapolate) the H6S bands (420, 443, 470, 510, 590 and 700 nm). The CDOM ( $a_s$ ), phytoplankton and detritus absorption ( $a_p$ ) coefficients were determined according to Mitchell et al.<sup>13</sup>. Fluorimetric Chla (FChla) was determined following the narrow band technique of Welschmeyer<sup>14</sup> (such as in Lutz et al.<sup>15</sup>). Phytoplankton pigments analyses were made with the High Liquid Performance Chromatography (HPLC) method according to Heukelen and Thomas<sup>16</sup>. The picoplankton cell concentration was determined with flow cytometry following methods reviewed by Marie et al.<sup>17</sup> with separation of heterotrophic bacteria (Bac), cyanobacteria (*Synechococcus* and *Prochlorococcus*) and picoeukaryote autotrophic cells. Uncertainty analyses were performed in each data set with comparisons of replicates analyzed at

different laboratories, using either similar or different technique. Possible outliers were eliminated in a quality control scheme.

### 2.2.1 Remote sensing reflectance ( $R_{rs}$ ) and MBR

The above-water remote sensing reflectance ( $R_{rs}$ ) was determined in two ways: averaging the radiometric measurements obtained from the CTD stations; and b) using a radiative transfer equation (RTE) to estimate  $R_{rs}$  using the measured IOP integrated in the first optical depth (1/diffuse attenuation coefficient ( $K_d$ )). The second alternative was determined for two reasons: first to compare with the measured  $R_{rs}$  as a closure analysis to evaluate the consistency between the two sets, and second to estimate the  $R_{rs}$  for the FI stations and add more sampled points to the analysis concerning the bio-optical variability. The RTE used was the approximation proposed by Morel et al.<sup>18</sup>:

$$R_{rs}(\lambda) \approx \frac{f(\lambda)}{Q(\lambda)} \frac{t_{(w,a)} t_{(a,w)}}{n_w^2} \frac{b_b(\lambda)}{a(\lambda)} \quad (1)$$

The  $f/Q$  factor is the environmental and bidirectional factor that relates  $R_{rs}$  to the IOP, varying with Chla and illumination conditions.  $t_{(w,a)}$  and  $t_{(a,w)}$  are the water-air and air-water transmittance factors and  $n_w$  is the refraction index of the sea water. The  $b_b/a$  is a simplified term of  $b_b/(a+b_b)$ , which may be valid for waters were  $b_b \ll a$ . Since there were waters collected also in enriched coastal areas, for which the  $b_b$  contribution may be high, the differences in the  $R_{rs}$  using  $b_b/(a+b_b)$  were analyzed and were within 5% (of normalized root mean square error (N\_RMSE)), so the simplified term was considered valid.

The MBR OC4<sup>1</sup> was implemented using the coefficients adjusted for its 6<sup>th</sup> version:

$$\log_{10}(\text{Chla}) = 0.3272 - 2.9940X + 2.7218X^2 - 1.2259X^3 - 0.5683X^4 \quad (2a)$$

$$X = \log_{10} \left( \frac{\max[R_{rs}(443), R_{rs}(490), R_{rs}(510)]}{R_{rs}(555)} \right) \quad (2b)$$

The second order variation of the MBR was analyzed in two ways, first by subtracting the measured MBR from the equivalent MBR of the polynomial fit associated to “true” measured Chla, resulting in an MBR\* (log scaled). However since some information of the spectral variability is lost when using a band ratio the second deviation index was obtained by the relative percent differences between the measured Chla and modeled Chla (Chla\*):  $\text{Chla}^* \text{RPD} = (\text{Chla}' - F\text{Chla}) / F\text{Chla} * 100$ .

### 2.2.3 Bio-optical indices

The bio-optical indices used to relate as possible sources of the second order variations of the MBR were the specific IOP:  $b_{bp}^*555$ ,  $a_{phy}^*443$  and  $a_{cdm}^*443$  and complementary indices of the particle size distribution (PSD), phytoplankton and bacterial community structure: a)  $b_{bp}$  spectral slope ( $\eta$ ) (from 443-555 nm); b) the CDOM spectral slope ( $S$ ) (from 300-555 nm) and the CDOM index<sup>5</sup> (equivalent to the  $a_{cdm}^*$  but just for CDOM); c) the fractions of the phytoplankton size groups estimated with the pigment ratios according to Vidulssi et al.<sup>19</sup>, and the size index of Bricaud et al.<sup>20</sup>; ratios of biomarker pigments to Chla, e.g. zeaxanthin (Zea) (Cyanophyceae) and prasinoxanthin (Pras) (Prasinophyceae); the ratio of photoprotective carotenoides (PPC) and photosynthetic carotenoides (PSC) to total carotenoides; and d) ratio of the concentration of heterotrophic bacteria (Bac) to Chla.

The analysis of relations between the MBR second order variations and bio-optical indices included: the separation of quartiles of the 25 % highest and lowest specific IOP to analyze the tendencies of over or underestimation (as in Loisel et al.<sup>6</sup>), and correlation analysis with spearman rank coefficients. In a final attempt to synthesize the bio-optical variability along the MV1102 transect a cluster analysis was applied using K-means to identify sub-sectors with similar bio-optical characteristics associated to the phytoplankton community size structure and biogeochemical dynamics.

### 3. RESULTS AND DISCUSSION

#### 3.1 Uncertainty Analysis

The measured  $R_{rs}$  and RTE had an average of 30% NRMSE with  $0.87 R^2$  for the ocean colour bands and 19% NRMSE with  $0.98 R^2$  for the band ratios (412; 443; 510/555). The highest differences were associated to adverse environmental conditions during the measurements, with high illumination variation due to cloudy conditions and rough seas (wind  $> 8 \text{ m.s}^{-1}$  and swells  $> 2.2 \text{ m}$ ). The differences of the ratios were much lower for favorable conditions ( $\sim 5\%$ ) and the RTE was considered reliable for the analysis of MBR variability. The coefficient of variation (CV) between the replicates of the  $a_s$  and  $a_p$  were 9-15% and 2-6%, respectively. The  $b_{bp}$  had generally low standard deviations (sd) within the first optical depth, but there were high sd associated to the 443 and 510 nm bands, which were removed from further analysis. In respect to the differences between the Chla retrieved with the fluorimetric (FChla) and HPLC analysis, the CV was high with an average of 40% higher retrieval for FChla. Nevertheless the  $R^2$  was high with 0.98 denoting a good consistency between the data sets. The major source of difference between the methods that could have caused an underestimation of the HPLC Chla was the solvent used for the pigment extraction. The FChla used 100% methanol which is known to have a higher extraction efficiency than the 90% acetone used in the HPLC analysis. This has been analyzed in previous works that also found differences of more than 30% solely due to the different solvents, applying the same method<sup>15</sup>. The possible underestimation of the HPLC Chla was confirmed by comparing the different Chla retrievals with the  $K_d490$  determined with the OCR profiler and comparing the  $K_d$  vs. Chla relation of Morel and Maritorea<sup>21</sup> (MM01). The FChla had a much closer fit with the MM01 relation. Thus, the FChla was used as the Chla reference measurement and the HPLC data set was used for the indices of the phytoplankton community (with the accessory pigment ratios).

#### 3.2. IOP distribution

The  $a_{phy443}$  ranged from 0.007-0.298  $\text{m}^{-1}$ ; the  $a_{cdm443}$  from 0.005-0.125  $\text{m}^{-1}$  and  $b_{bp555}$  from 0.0011-0.0043  $\text{m}^{-1}$ . Their distribution in relation to Chla was within the dispersion of data collected from other cruises and around the mean fits proposed in other works (Figure 2).

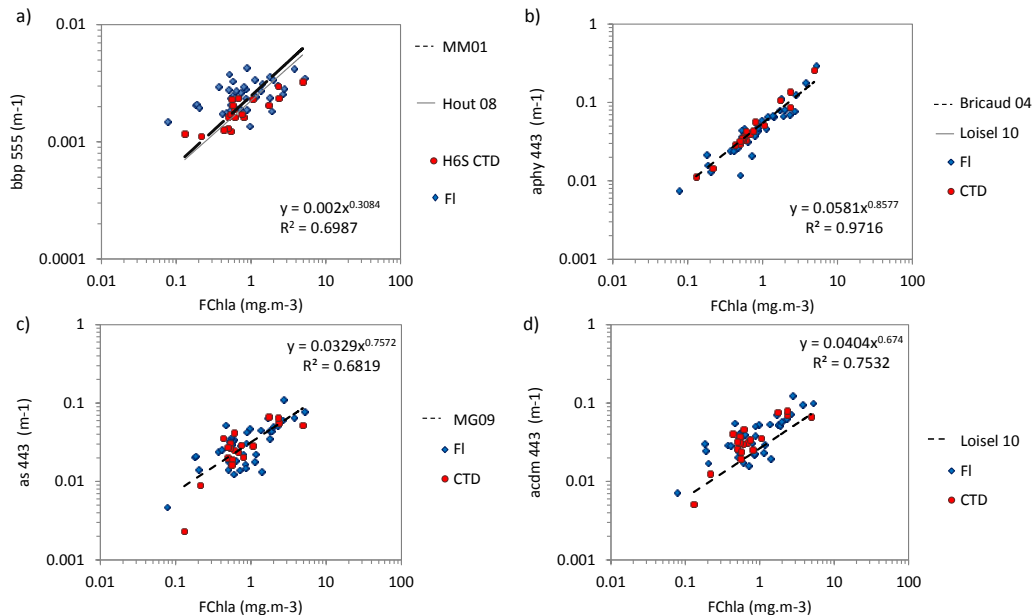


Figure 2: Dispersion graphs of the bio-optical properties vs. Chla, red dots are CTD stations and blue diamonds are FI stations: a)  $b_{bp\ 555}$ , with the Hout et al.<sup>22</sup> (Hout 08) and Morel and Maritorea<sup>21</sup> (MM01) fits for  $b_{bp}$ ; b)  $a_{phy\ 443}$  with the Bricaud et al.<sup>20</sup> (Bricaud 04) and Loisel et al.<sup>6</sup> (Loisel 10) fits; c)  $a_s\ 443$  with the Morel and Gentili<sup>5</sup> (MG09) fit; and d)  $a_{cdm\ 443}$  with the for  $a_s$  and Loisel et al.<sup>6</sup> (Loisel 10) fit. All axes are in log scale.

### 3.3 Quartile Analysis

The first analysis to verify the sources of biases of the OC4 in respect to the bio-optical variability, was dividing the  $a_{\text{phy}}^*$ ,  $b_{\text{bp}}^*$  and  $a_{\text{cdm}}^*$  into the highest and lowest quartile. As in Loisel et al.<sup>6</sup> there was a trend of overestimation of the OC4 related to the highest quartile of the specific IOP and underestimation with the lowest values (Figure 3). For the highest  $a_{\text{phy}}^*$  stations the OC4 overestimated in -32% (RPD) and underestimated in 33% for the lowest. For the highest  $b_{\text{bp}}^*$  the OC4 overestimated in 24% and underestimated in -13% for the lowest, and for the highest  $a_{\text{cdm}}^*$  the OC4 overestimated 26%, and had a very low underestimation for the lowest quartile (-0.9 %).

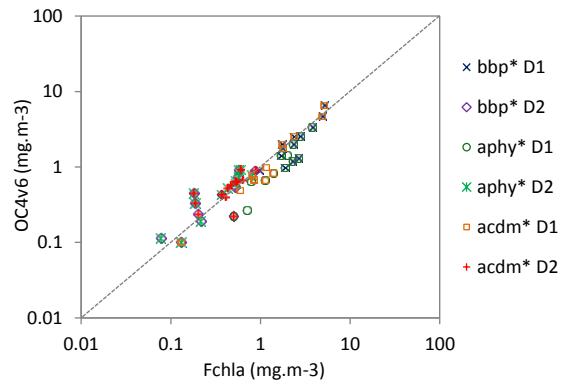


Figure 3: OC4v6 vs. measured Chl a (Fchl a) with the highest (D2) and lowest (D1) quartile of each specific IOP:  $b_{\text{bp}}^*$ ,  $a_{\text{phy}}^*$  and  $a_{\text{cdm}}^*$ .

### 3.4 Correlation Analysis

For the correlation analysis the MBR\* had lower correlations than the Chl a\*, probability due to the loss of information on the spectral variability when using the  $R_{\text{rs}}$  ratios, and both were negatively correlated as they have inverse relations (-0.68) (Table 1). The MBR\* was negatively correlated with the CDOM index (CI) (-0.42) and  $a_{\text{phy}}^*$  (-0.44). Higher CI and  $a_{\text{phy}}^*$  both cause higher absorption in the blue bands diminishing the MBR, which would cause an overestimation of OC4 Chl a. The MBR\* was also positively correlated with the CDOM spectral slope  $S$  (0.26). The higher  $S$  occurred when there was a very low CDOM absorption in the visible range and a rapid increase towards the ultraviolet. The lower CDOM absorption from 443-555 nm caused then a higher MBR, which underestimated Chl a. There was also a slight positive correlation between the MBR\* and  $b_{\text{bp}}$  spectral slope ( $\eta$ ) (0.23), which may be related to a greater influence of smaller particles on the  $b_{\text{bp}}$ , enhancing the  $R_{\text{rs}}$  at shorter bands, and also retrieving a higher MBR. In respect to the Chl a\* the  $a_{\text{phy}}^*$  had the highest positive correlation (0.73) followed by CI (0.52),  $a_{\text{cdm}}^*$  (0.42) and  $b_{\text{bp}}^*$  (0.38) (Table 1). In the same way as previously discussed higher  $a_{\text{phy}}^*$  phytoplankton assemblages have higher absorption in the shorter bands, causing an overestimation of the Chl a with the MBR OC4, and vice-versa. Higher CDOM and  $a_{\text{cdm}}^*$  have a similar effect. The higher  $b_{\text{bp}}^*$  has an effect of increasing the  $R_{\text{rs}}$  especially at the longer bands (555), which in turns also diminishes the MBR and causes an overestimation of the Chl a. Loisel et al.<sup>6</sup> also found similar relations between the Chl a biases and the  $a_{\text{phy}}^*$ ,  $a_{\text{cdm}}^*$  and  $b_{\text{bp}}^*$ . They also discussed that the impact of each specific IOP on the MBR will depend on their range of variability, and when considering the same range of variability of each specific IOP, i.e., the  $a_{\text{cdm}}^*$  actually would have the highest impact on the MBR and OC4 biases, due to the exponential nature of its spectral absorption.

In respect to the bacterial and phytoplankton indices of the community structure, the Chl a\* was positively correlated with all the indices that co-varied positively with  $a_{\text{phy}}^*$  and  $b_{\text{bp}}^*$ , which were the picoplankton fraction (0.40), the heterotrophic bacterial proportion (Bac\*) (0.45), and the PPC\* (0.51), which was highly correlated to Zea\* (0.90) (as expected in waters with Cyanophyceae<sup>20</sup>), Pras\* (0.44) and Gyr\* (0.45). High  $a_{\text{phy}}^*$  was thus associated with dominance of small picophytoplankton cells with an assemblage characterized by dominance of cyanobacteria (indexed by Zeaxanthin) (mostly of *Synechococcus* and *Prochlorococcus* as counted in the flow cytometry), in association with

Prasinophytes (indexed by Prasinonanthin), which are very small Chlorophytes (~0.95  $\mu\text{m}$ ), and some occurrence of Gyrodinium sp. (indexed by Gyroxanthin diester, Gry). This last group is actually a relatively large sized group (20-60 $\mu\text{m}$ ) that showed high correlations with the  $b_{\text{bp}}^*$  (0.85) and  $a_{\text{phy}}^*$  (0.60), probably because it occurred in low concentrations, as the ratios of Gry were generally low, and were associated with higher abundance of bacteria (0.88) and Cyanophyceas (0.65), which may in fact have high  $a_{\text{phy}}^*$  and  $b_{\text{bp}}^*$ . On the other hand the Chla\* was negatively correlated with the microphytoplankton fraction (-0.28), Chlc12\* (-0.34), and PSC\* (-0.51) indicator of diatoms and some nano groups, which were associated to lower  $a_{\text{phy}}^*$  and  $b_{\text{bp}}^*$ . The Hex\* (hexa-fucoxanthin) which is an indicator of some Haptophytes (including Coccolithophorids) and dinoflagellates, was not encountered in high proportions but did show some correlation with the  $\text{bbp } \eta$  (0.32) and a high correlation with the nano fraction (0.95).

Table 1: Spearman Correlation Rank for the second order MBR variation (MBR\*) and Chla bias (Chla\*) and specific bio-optical properties:  $a_{\text{phy}}^*$ ,  $b_{\text{bp}}^*$ ,  $b_{\text{bp}}$  spectral slope  $\eta$ ,  $a_{\text{cdm}}^*$ , CDOM index (CI), CDOM spectral slope  $S$ , picoplankton fraction (nPF), nano (nPF) and microplankton (mPF), phytoplankton size index (SI), proportion of heterotrophic bacteria (Bac\*), percentage of Prochlorococcus (Proch), photosynthetic carotenoids (PSC\* ) and photoprotective carotenoids ratio (PPC\*); and pigment ratios with TChla: Hexa fucoxanthin (Hex), Zeaxanthin (Zea), Chlb, Chlc12, Prasinonanthin (Pras) and Gyroxanthin diester (Gyr). The significant coefficients ( $p < 0.05$ ) are in bold.

	Fchla	MBR*	Chla*	bbp*	bbp n	acdm*	CI	aphy*	[pPF]	[nPF]	[mPF]	SI	Bac*	Proch	[PSC]*	[PPC]*
Fchla	1.00															
MBR*	-0.13	1.00														
Chla*	<b>-0.42</b>	<b>-0.88</b>	1.00													
bbp*	<b>-0.87</b>	0.09	<b>0.38</b>	1.00												
bbp n	<b>-0.44</b>	0.23	-0.14	<b>0.27</b>	1.00											
acdm*	<b>-0.54</b>	-0.08	<b>0.42</b>	<b>0.46</b>	0.14	1.00										
CI	<b>-0.32</b>	<b>-0.52</b>	<b>0.53</b>	0.17	0.15	<b>0.77</b>	1.00									
S (as)	-0.07	<b>0.26</b>	<b>-0.37</b>	0.01	0.19	-0.23	-0.22									
aphy*	<b>-0.68</b>	<b>-0.44</b>	<b>0.73</b>	<b>0.56</b>	0.17	0.18	<b>0.31</b>	1.00								
[pPF]	<b>-0.79</b>	-0.01	<b>0.40</b>	<b>0.73</b>	0.16	0.24	0.04	<b>0.69</b>	1.00							
[nPF]	-0.17	-0.10	0.04	0.12	<b>0.32</b>	0.06	0.03	0.05	-0.04	1.00						
[mPF]	<b>0.74</b>	0.03	<b>-0.28</b>	<b>-0.64</b>	<b>-0.36</b>	-0.24	-0.07	<b>-0.59</b>	<b>-0.82</b>	<b>-0.40</b>	1.00					
SI	<b>0.74</b>	0.03	<b>-0.31</b>	<b>-0.67</b>	<b>-0.31</b>	<b>-0.29</b>	-0.05	<b>-0.56</b>	<b>-0.85</b>	<b>-0.36</b>	1.00	1.00				
Bac*	<b>-0.92</b>	-0.05	<b>0.45</b>	<b>0.87</b>	<b>0.41</b>	<b>0.48</b>	<b>0.27</b>	<b>0.64</b>	<b>0.75</b>	0.16	<b>-0.74</b>	<b>-0.76</b>	1.00			
% Proch	<b>-0.45</b>	0.24	0.06	<b>0.44</b>	0.20	<b>0.37</b>	0.13	0.18	<b>0.35</b>	<b>-0.33</b>	-0.24	-0.24	<b>0.52</b>	1.00		
[PSC]*	<b>0.54</b>	0.25	<b>-0.51</b>	<b>-0.51</b>	-0.03	<b>-0.28</b>	<b>-0.29</b>	<b>-0.55</b>	<b>-0.61</b>	0.23	<b>0.39</b>	<b>0.43</b>	<b>-0.61</b>	<b>-0.48</b>	1.00	
[PPC]*	<b>-0.54</b>	-0.25	<b>0.51</b>	<b>0.51</b>	0.03	<b>0.28</b>	<b>0.29</b>	<b>0.55</b>	<b>0.61</b>	-0.23	<b>-0.39</b>	<b>-0.43</b>	<b>0.61</b>	<b>0.48</b>	-1.00	1.00
[Hex]	-0.20	-0.05	0.02	0.17	<b>0.32</b>	-0.01	-0.04	0.10	0.08	<b>0.95</b>	<b>-0.51</b>	<b>-0.47</b>	0.21	<b>-0.33</b>	0.20	-0.20
[Zea]	<b>-0.71</b>	-0.21	<b>0.55</b>	<b>0.65</b>	0.24	<b>0.42</b>	<b>0.37</b>	<b>0.58</b>	<b>0.70</b>	0.01	<b>-0.60</b>	<b>-0.62</b>	<b>0.78</b>	<b>0.47</b>	<b>-0.90</b>	<b>0.90</b>
[Chl b]	-0.33	-0.08	0.17	0.32	0.04	-0.08	-0.21	<b>0.34</b>	<b>0.59</b>	<b>0.42</b>	<b>-0.61</b>	<b>-0.60</b>	<b>0.32</b>	-0.24	-0.01	<b>0.01</b>
[Chl c12]	<b>0.76</b>	0.00	<b>-0.34</b>	<b>-0.66</b>	-0.21	<b>-0.33</b>	-0.15	<b>-0.65</b>	<b>-0.89</b>	0.13	<b>0.70</b>	<b>0.73</b>	<b>-0.70</b>	<b>-0.46</b>	<b>0.63</b>	<b>-0.63</b>
[Pras]	<b>-0.77</b>	0.02	<b>0.37</b>	<b>0.75</b>	<b>0.43</b>	<b>0.30</b>	0.09	<b>0.53</b>	<b>0.68</b>	0.16	<b>-0.68</b>	<b>-0.70</b>	<b>0.81</b>	<b>0.36</b>	<b>-0.44</b>	<b>0.44</b>
[Gyr]	<b>-0.94</b>	0.12	<b>0.32</b>	<b>0.85</b>	<b>0.44</b>	<b>0.49</b>	<b>0.26</b>	<b>0.60</b>	<b>0.79</b>	0.15	<b>-0.75</b>	<b>-0.77</b>	<b>0.88</b>	<b>0.40</b>	<b>-0.45</b>	<b>0.45</b>

The sources of variation of the  $b_{\text{bp}}^*$  is rather questionable as there is not yet a consensus on what are the main sources of  $b_{\text{bp}}$  in oceanic waters<sup>22</sup>. Phytoplankton cells actually have low  $b_{\text{bp}}$  efficiency. Nevertheless, the pico fraction showed a high correlation with the  $b_{\text{bp}}^*$  (0.77). It may be true that the size structure of the phytoplankton community may co-vary with the size structure of the bulk particle assemblage (both living and non-living) and that sub-micron detritus, which has been cited as a possible major source of oceanic  $b_{\text{bp}}$ <sup>7</sup>, could be more abundant in picoplankton dominated waters. Another important source of  $b_{\text{bp}}$  could also be from heterotrophic bacteria<sup>7</sup> and in fact Bac\* had the highest correlation with  $b_{\text{bp}}^*$  (0.85). The Bac\* also had a positive correlation with the CDOM index and  $a_{\text{cdm}}^*$  (0.49 and 0.42, respectively), which may also indicate higher level of degradation processes associated to these assemblages, which would “produce” more sub-micron detritus and CDOM due to higher bacterial activity.

### 3.5 Cluster Analysis

The K-means cluster analysis was applied to group the stations with similarities of the specific IOP and phytoplankton assemblages, using:  $a_{phy}^*$ ,  $b_{bp}^*$ ,  $a_{cdm}^*$ , PPC\* and PSC\*. It was possible to separate four groups of stations. Group 1 had the highest  $a_{phy}^*$ ,  $b_{bp}^*$  and PPC\* (Figure 4). It was characterized by oligo-mesotrophic waters (0.08-0.60mg.m<sup>-3</sup>) dominated by picoplankton (57%) (Table 2) and grouped the stations of the Southeast Atlantic under influence of the SAG and BEN, and one station in the SCAZ and the Chilean coast. The OC4 Chla was mostly overestimated with a 32% RPD. The assemblage was characterized by dominance of Cyanophyceas (*Synechococcus* and *Prochlorococcus*) which have high  $a_{phy}^*$  and are widely distributed especially in oligotrophic waters of the subtropical Gyres<sup>8,20</sup>. There were also Prasinophytes which have also high  $a_{phy}^*$ , and high abundance of Bac\* which may have contributed to high  $b_{bp}^*$ . Group 2 had the lowest  $a_{phy}^*$  and  $b_{bp}^*$  and highest PPC\* and was characterized by meso-eutrophic waters (1.67±0.76 mg.m<sup>-3</sup>) dominated by microplankton (53%). The stations were mostly from the Chilean coast and 4 stations from the SCAZ, and were associated to the highest underestimations of Chla (-33%). The southern Chilean Coast is actually a highly productive system with evidence of higher abundance of diatoms that may be stimulated by penetrations of HNLC waters of the Southern Ocean into the iron enriched coast<sup>10</sup>. Group 3 had similar values as group 2, but with a higher  $a_{phy}^*$ , which characterized nanoplankton dominated waters (49%) with mesotrophic waters (0.67 ±0.28 mg.m<sup>-3</sup>) of the SAZC and Chilean coast. Group 4 had similar  $b_{bp}^*$  and  $a_{phy}^*$  as group 3 and was also characterized by nanoplankton dominated waters (41%), but with lower  $a_{cdm}^*$ . It grouped meso-eutrophic stations (1.76±1.53 mg.m<sup>-3</sup>) of the SACZ and Patagonian Shelf (PSE). The PSE is a highly productive system and a higher contribution of microplankton would be expected, however other studies conducted in this complex region have also found dominance of nano groups and even nano sized diatoms (Vivian Lutz personal communication). The lower  $a_{cdm}^*$  could be partly associated to a higher stratified environment as was observed within the vertical profile of the CTD stations at the PSE. Groups 3 and 4 had closer matches with the OC4 model, with a slight tendency of overestimating for G3 due mainly to higher  $a_{phy}^*$ , and underestimating of G4 due to lower  $a_{cdm}^*$ .

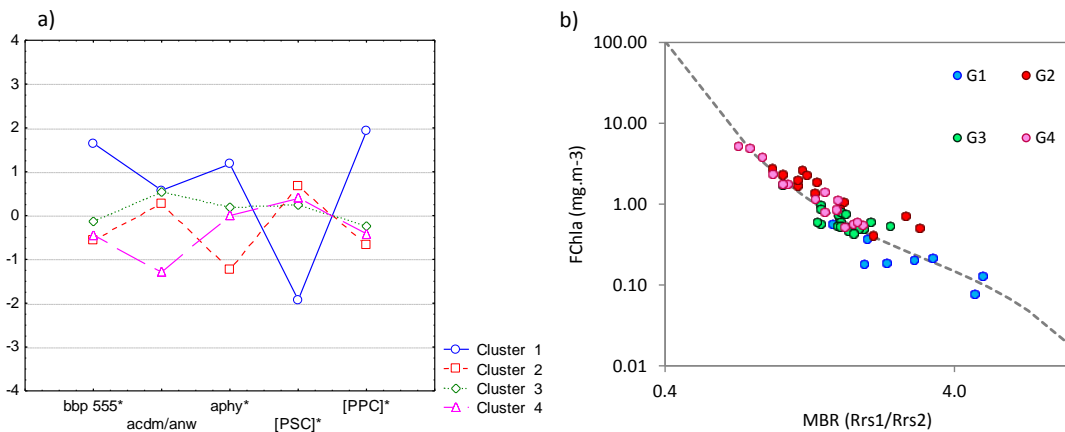


Figure 4: a) Mean normalized values of the  $bbp^*$ ,  $a_{phy}^*$ ,  $a_{cdm}^*$ , PPC and PSC for each Cluster or Group (1, 2, 3 and 4); and b) FChla vs. the MBR with the OC4v6 fit (dashed line) and stations marked by each group.

Table 2: Mean and standard deviation of the FChla, Chla\* (RPD),  $bbp^*$ ,  $a_{phy}^*$ ,  $a_{cdm}^*$ , PPC\*, PSC\*, and pico, nano and micro fraction for each group of the cluster analysis.

	Fchla	Chla*	$bbp^*$	$a_{phy}^*$	$a_{cdm}^*$	PPC*	PSC*	Pico	Nano	Micro
G1	0.28 ±0.16	0.32 ±0.50	0.009 ±0.004	0.079 ±0.019	0.503 ±0.087	0.54 ±0.12	0.46 ±0.12	0.57	0.30	0.14
G2	1.67 ±0.76	-0.33 ±0.18	0.002 ±0.001	0.039 ±0.009	0.471 ±0.058	0.12 ±0.03	0.88 ±0.03	0.13	0.34	0.53
G3	0.67 ±0.28	0.08 ±0.21	0.003 ±0.001	0.062 ±0.007	0.499 ±0.058	0.19 ±0.06	0.81 ±0.06	0.31	0.49	0.20
G4	1.76 ±1.53	-0.08 ±0.18	0.002 ±0.001	0.059 ±0.010	0.314 ±0.049	0.16 ±0.06	0.84 ±0.06	0.25	0.41	0.34

Group 1 (G1): n= 10; Group 2 (G2): n= 12; Group 3 (G3): n= 20 and Group 4 (G4): n= 16.

#### 4. FINAL CONSIDERATIONS

The relations between the second order variations of the MBR\* and the Chla biases of the OC4 fit and the specific IOP were consistent with previous investigations. High  $a_{\text{phy}}^*$ ,  $b_{\text{bp}}^*$  and  $a_{\text{cdm}}^*$  were associated with overestimation by OC4 and low specific IOP with underestimation. The present work also examined the relations between the specific IOP and indices of the bacterial and phytoplankton community structure, and the relations were also found to be consistent with previous studies. High  $a_{\text{phy}}^*$  was associated with pico and small nano phytoplankton assemblages and low  $a_{\text{phy}}^*$  to microplankton dominance. High  $b_{\text{bp}}^*$  was associated with picoplankton dominance and higher heterotrophic bacteria (HB) abundance. The HB could be a significant contributor to the  $b_{\text{bp}}^*$ , but also be related to higher concentrations of submicron detritus particles, due to higher bacterial decomposition. The bio-optical variability within the surface layer of the cruise transect was well synthesized into four groups of stations with specific IOP and phytoplankton assemblages.  $a_{\text{phy}}^*$  and  $b_{\text{bp}}^*$  co-varied and defined the highest differences within the groups, while  $a_{\text{cdm}}^*$  had a more complex mode of variation due to different biogeochemical processes governing its variability in each region. There were some relations between higher  $a_{\text{cdm}}^*$  and pico dominated waters, and between lower  $a_{\text{cdm}}^*$  and more stratified stations of the PSE. The bio-optical groups were mostly linked to the different biogeochemical provinces, but there were also similarities between some stations of the BEG, SACZ, Chilean Coast and Patagonian Shelf. This reveals the complexity in partitioning the region into bio-optical provinces, as the main variabilities were linked to similar assemblages that co-occurred in different provinces. The present work contributed with analysis of the main sources of second order variations of the MBR and characterization of the bio-optical variability within the study region, associated with indices of the phytoplankton community structure.

#### ACKNOWLEDGMENTS

The authors gratefully acknowledge the participants of the MV1102 and all institutions and researchers involved in the data collection and analysis: the National Aeronautics and Space Administration (NASA), *Instituto Nacional de Pesquisas Espaciais* (INPE), Scripps Institution of Oceanography (SIO), *Universidade de São Paulo* (USP), *Universidade Federal do Rio de Janeiro* (UFRJ), *Instituto Nacional de Investigación y Desarrollo Pesquero* (INIDEP) and *Coordenação de Aperfeiçoamento Pessoal* (CAPES). NASA supports R. Frouin under grants NNX11AR07G and NNX11AI36G.

#### REFERENCES

- [1] O'Reilly, J. E., Maritorena, S., Mitchell, B. G., Siegel, D. A., Carder, K. L., Garver, S. A., Kahru, M., and McClain C. R., "Ocean color chlorophyll algorithms for SeaWiFS," *J. Geophys. Res.* 103(C11), 24,937–24,953 (1998).
- [2] Morel A. and Prieur, L., "Analysis of variations in ocean color". *Limnol. Oceanogr.*, 22(4), 709-722 (1997).
- [3] Szeto, M., Werdell, J., Moore, T. S., and Campbell, J. W., "Are the world's oceans optically different?," *J. Geophys. Res.*, 116, 1-14 (2011).
- [4] Brown, A., Huot, Y., Werdell, P. J., Gentili, B. and Claustre, H., "The origin and global distribution of second order variability in satellite ocean color and its potential applications to algorithm development," *Remote Sens. Environ.* 112(12), 4186–4203 (2008).
- [5] Morel, A., and Gentili, B., "The dissolved yellow substance and the shades of blue in the Mediterranean Sea," *Biogeosciences* 6(11), 2625–2636 (2009).
- [6] Loisel, H., Lubac, B., Dessailly, D., Duforet-Gaurier, L., Vantrepotte, V., "Effect of inherent optical properties variability on the chlorophyll retrieval from ocean color remote sensing: an in situ approach," *Opt. Express*, 18 (20) 20949-59 (2010).
- [7] Stramski, D., Boss, D., E. Bogucki, D., and Voss, K. J., "The role of seawater constituents in light backscattering in the ocean," *Prog. Oceanogr.*, 61, 27–56 (2004).

- [8] Ciotti, A., A. M. Lewis, and J. Cullen. "Assessment of the relationships between dominant cell size in natural phytoplankton communities and the spectral shape of the absorption coefficient," *Limnol. Oceanogr.*, 47(2) 404-417, (2002).
- [9] Longhurst, A., [Ecological geography of the sea], 2nd ed., Academic Press (2007)
- [10] Romero O. and Hebbeln D., "Biogenic silica and diatom hantocoenosis in surface sediments below the Peru Chile Current: controlling mechanisms and relationship with productivity of surface waters," *Marine Micropaleontology* 48, 71-90 (2003)
- [10] Mueller, J. L., et al., "Ocean Optics Protocols For Satellite Ocean Color Sensor Validation," Revision 4, Volume III, 78p. National Aeronautical and Space Administration, Goddard Space Flight Space Center, Greenbelt, Maryland 20771, January, (2003).
- [12] Dana R. A. and Maffione, D. R., "Instruments and methods for measuring the backward-scattering coefficient of ocean waters," *Applied Optics*, vol 36 (24) 6057-67 (1997).
- [13] Mitchell, B.G., "Algorithms for determining the absorption coefficient of aquatic particulates using the quantitative filter technique (QFT)," *Ocean Optics X*. 137-148, (1990).
- [14] Welschmeyer, N., "Fluorometric chlorophyll a analysis in presence of Chlorophyllb and pheopigments," *Limnol. Oceanogr.* 39 (8) 1985-1992 (1994).
- [15] Lutz, V., Segura, V., Dogliotti, A. I., Gagliardini, D. A., Bianchi, A. A., Balestrini C. F., "Primary production in the Argentine Sea during spring estimated by field and satellite models," *J. Plank. Res.* 32 (2) 181-195 (2010).
- [16] Heukelen L. V. and Thomas, C. S., "Computer-assisted high-performance liquid chromatography method development with applications to the isolation and analysis of phytoplankton pigments," *J. Chromat.*, 910, 31-49 (2001)
- [17] Marie, D., Simon, D., N., Vaulot, D., [Phytoplankton cell counting by flow cytometry], In R. A. Andersen. (eds), *Algal Culturing Techniques*. Academic Press, Elsevier, San Diego, California, pp. 253-267 (2005)
- [18] Morel. A., Antoine, D., Gentili, B., "Bidirectional reflectance of oceanic waters: accounting for Raman emission and varying particle scattering phase function," *Applied Opt.* 41 (30), 6289-6306 (2002).
- [19] Vidussi, F., Claustre, F., H., Manca, B. B., Luchetta, A. and Marty, J. C., "Phytoplankton pigment distribution in relation to upper thermocline circulation in the eastern Mediterranean Sea during winter," *J. Geophys. Res.* 106(C9), 19,939- 19,956 (2001).
- [20] Bricaud, A., Claustre, H., Ras, J. and Oubelkheir, K., "Natural variability of phytoplankton absorption in oceanic waters: Influence of the size structure of algal populations," *J. Geophys. Res.* 109(C11), C11010 (2004).
- [21] Morel, A. and Maritorena S., "Bio-optical properties of oceanic waters: A reappraisal," *J. Geophys. Res.* 106, 7163-7180 (2001).
- [22] Huot, Y., Morel, A., Twardowski, M. S., Stramski, D. and Reynolds, R. A., "Particle optical scattering along a chlorophyll gradient in the upper layer of the eastern South Pacific Ocean," *Biogeosciences* 5(2), 495-507 (2008).